

# LOCAL AND REGIONAL CHARACTERISATION OF THE DIURNAL MOUNTAIN WIND SYSTEMS IN THE GUADARRAMA MOUNTAIN RANGE (SPAIN)

JON A. ARRILLAGA <sup>(1)</sup>, DARÍO CANO <sup>(2)</sup>, MARIANO SASTRE <sup>(1)</sup>, CARLOS ROMÁN-CASCÓN <sup>(1, 3)</sup>, GREGORIO MAQUEDA <sup>(1)</sup>, GEMA MORALES <sup>(4)</sup>, SAMUEL VIANA <sup>(4)</sup>, ROSA M. INCLÁN <sup>(5)</sup>, J. FIDEL GONZÁLEZ-ROÚCO <sup>(1)</sup>, EDMUNDO SANTOLARIA <sup>(1)</sup>, LUIS DURÁN <sup>(6)</sup>, CARLOS YAGÜE <sup>(1)</sup>

(1) Universidad Complutense de Madrid, Madrid, Spain ([jonanarr@ucm.es](mailto:jonanarr@ucm.es)). (2) Madrid-Barajas Adolfo Suárez Airport Office, AEMET, Madrid, Spain. (3) Univ. Grenoble Alpes, CNRS, IRD, Grenoble INP, IGE, F-38000 Grenoble, France. (4) AEMET, Madrid, Spain. (5) Centro de Investigaciones Energéticas, Medioambientales y Tecnológicas (CIEMAT), Madrid, Spain. (6) InterMET Sistemas y Redes S.L.U., Madrid, Spain.

## 1. OBSERVATIONAL SITE

La Herrería observational site (40.58 °N, 4.13 °W, 920 m asl) is located at the foot of the Guadarrama mountain range (Fig. 1) and at ≈ 50 km from the city of Madrid.

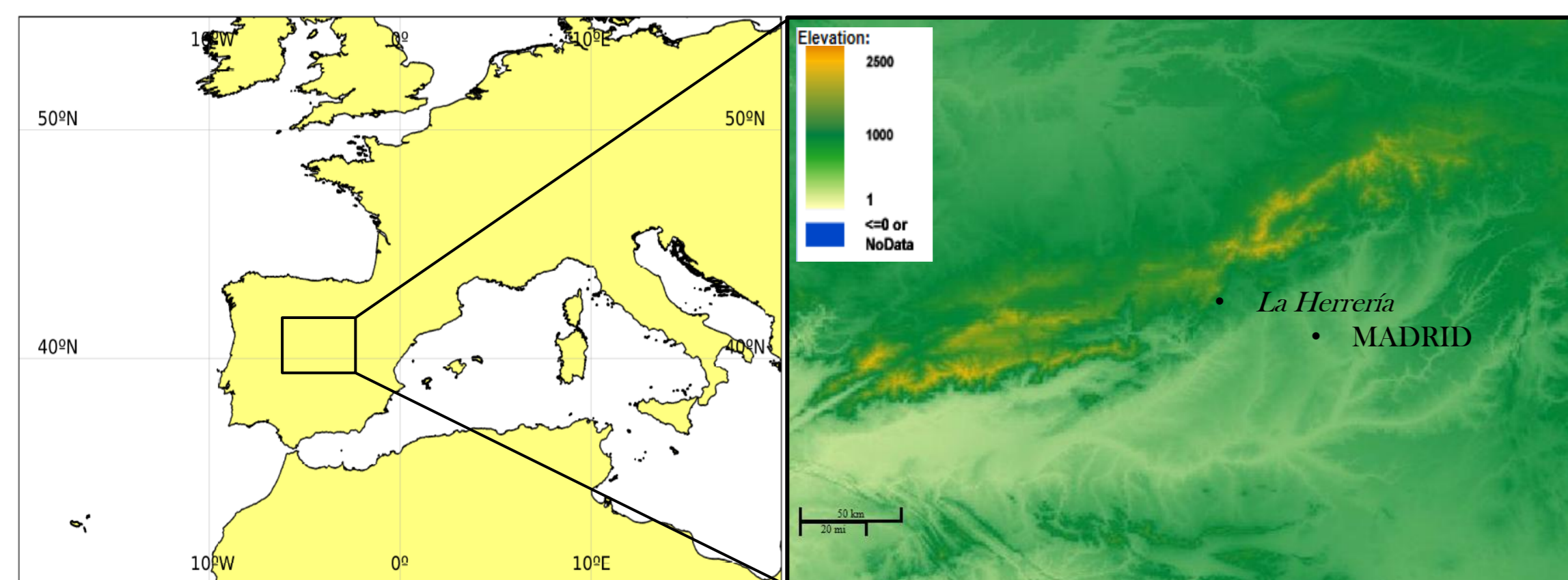


Figure 1. Location of La Herrería site and the city of Madrid (Spain). The source of topography data is ASTER GDEM (METI, NASA).

Atmospheric instrumentation in the 10-m tower has been installed in order to study the evolution of the lower atmosphere under the influence of the diurnal mountain wind systems. La Herrería is part of the Guadarrama Monitoring Network (GUMNet; [www.ucm.es/gumnet/](http://www.ucm.es/gumnet/)).

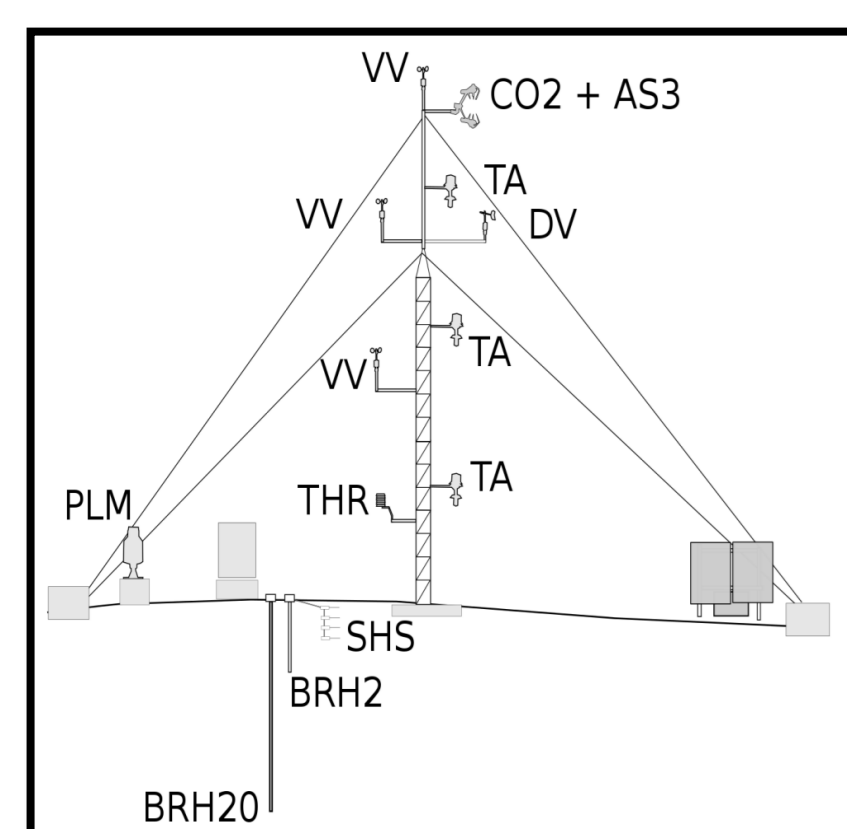


Figure 2. Instrumentation in the 10-m fixed tower. It contains wind-speed (VV) and air-temperature sensors (TA) at 3 different levels. A thermohygrometer (THR) and a wind vane (DV) are also included. This configuration is complemented with an in-situ open-path mid-infrared absorption gas analyzer, integrated with a three dimensional sonic anemometer (CO2 + AS3). Data are continuously recorded from June 2016. Moreover, the station includes two experimental boreholes (BRH20 and BRH2), soil temperature and moisture sensors inserted in a trench (SHS) and a pluviometer (PLM), but these data are not available for the temporal range spanned in this work, except for the trench.

## 2. RESEARCH INTEREST

The soil underwent a severe drying up over Summer 2016 (07/06/2016 – 13/09/2016):

RQ1: HOW DOES THIS DRYING OUT AFFECT THE DIURNAL MOUNTAIN WIND SYSTEM AND THE ASSOCIATED TURBULENCE?

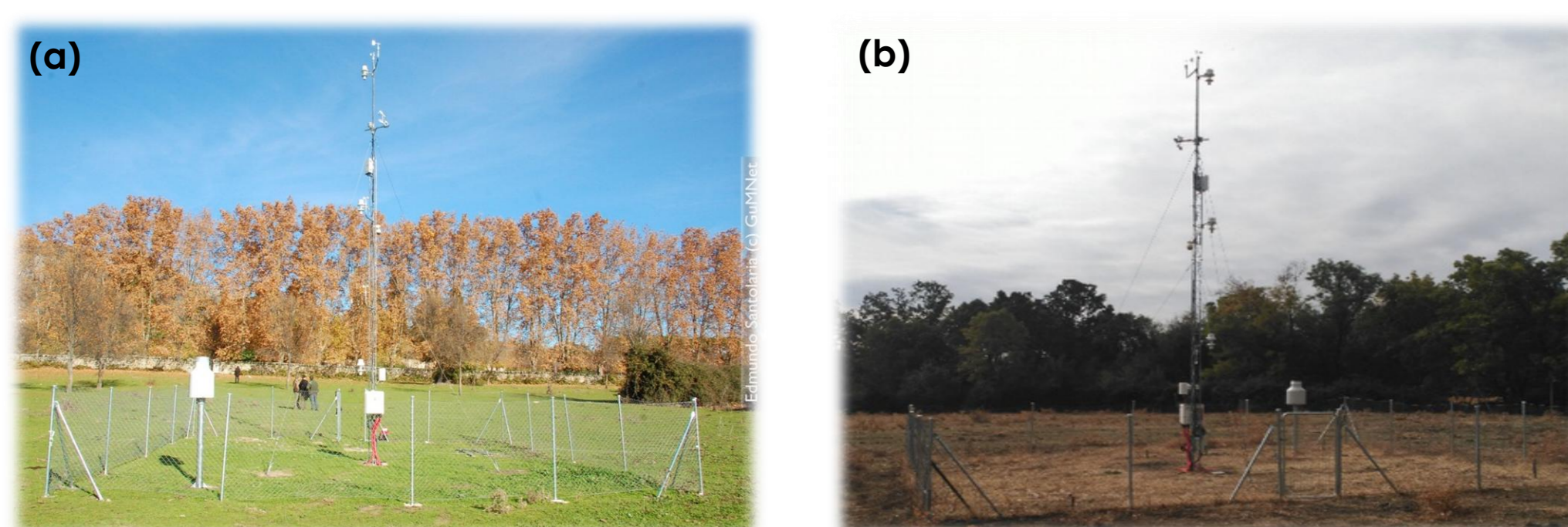


Figure 3. Photography of La Herrería site (a) under wet conditions and (b) under very dry conditions.

When the observed tail wind exceeds 10 kt in the Adolfo Suárez Madrid Barajas Airport, the runway configuration (NORTH-SOUTH) needs to be modified:

RQ2: WHAT IS THE ROLE OF THE MOUNTAIN BREEZES IN THE RUNWAY-CONFIGURATION ISSUE?

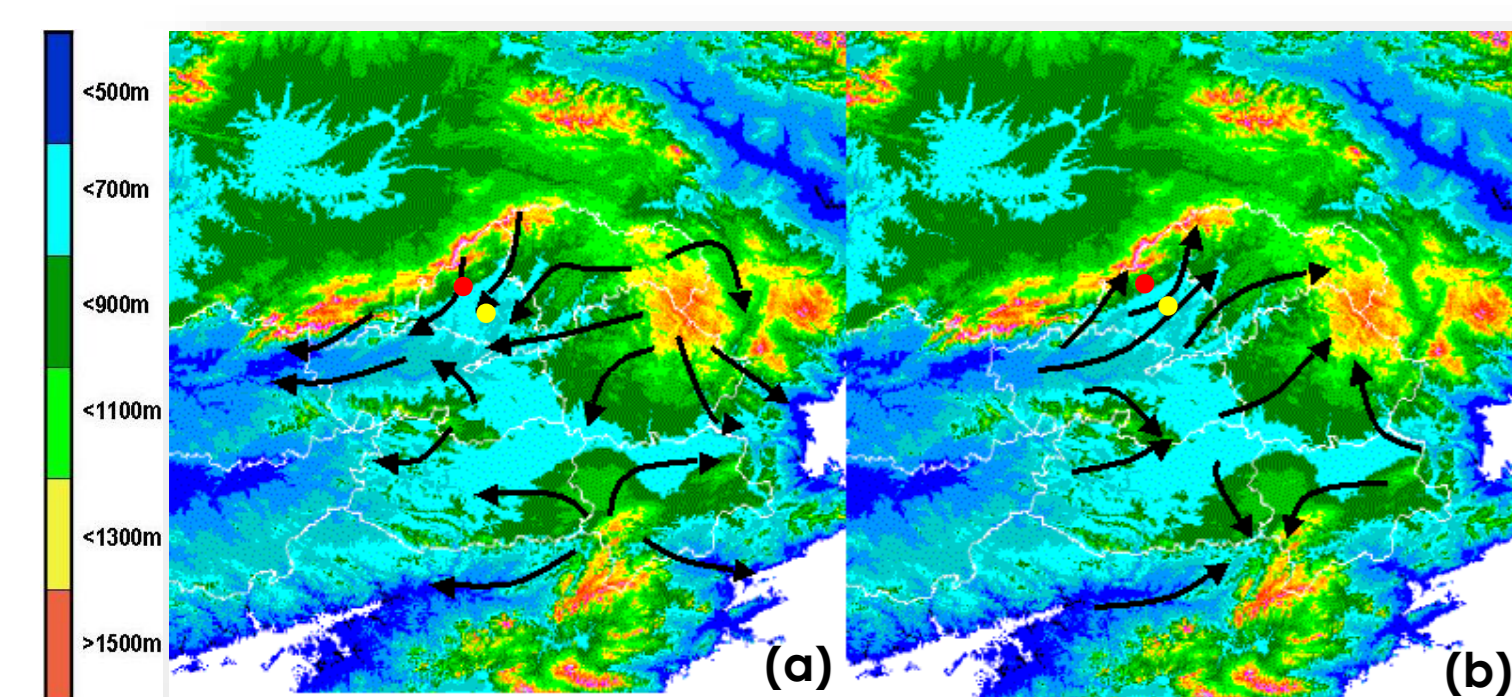


Figure 4. Diagram of the thermal mountain winds (a) during night-time and (b) during daytime. The location of La Herrería and the airport of Madrid are pointed with a red and a yellow dot respectively.

## 3. SUMMER 2016: SEVERE DRYING OUT

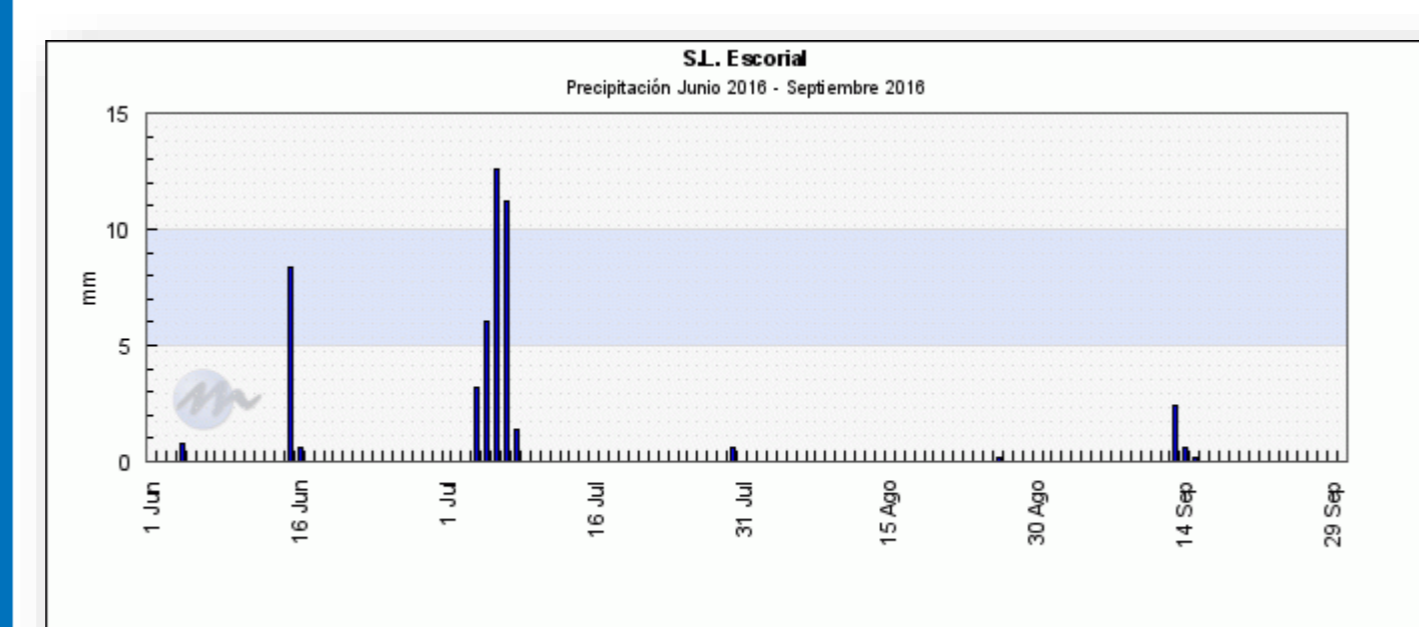


Figure 5. Recorded precipitation from 01/06/2016 until 30/09/2016 at San Lorenzo El Escorial, 5 km from La Herrería Site (Source: MeteoClimatic).

We compute the Bowen ratio ( $\beta$ ) throughout Summer 2016 for the available data (07/06/2016 – 13/09/2016):

$$\beta_{DAY} = \frac{SH_{daily\ mean}}{LH_{daily\ mean}}$$

The Bowen ratio increases throughout the summer (Fig. 5) particularly due to the lack of precipitations in the second half of the season (Fig. 4) and the very high temperatures (not shown here).

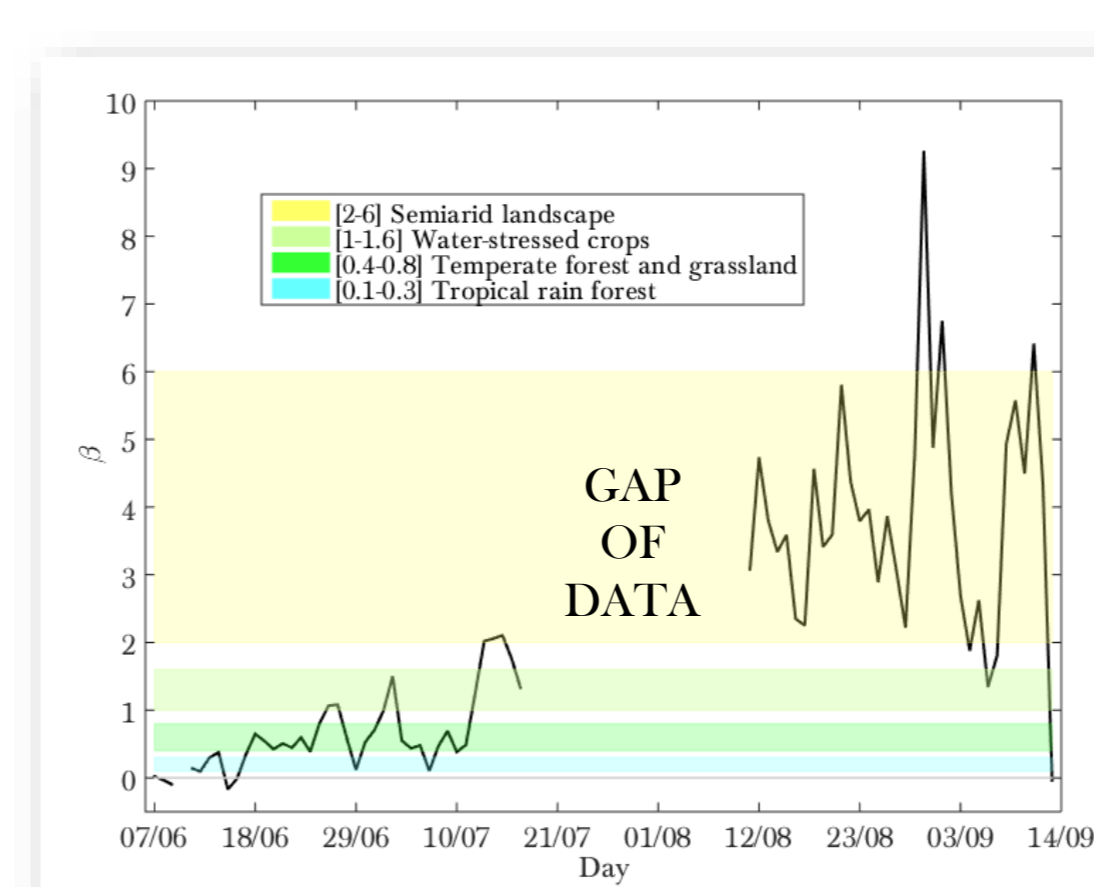


Figure 6. Evolution of the mean daily Bowen ratio over the summer. We include shaded areas of typical values for semiarid landscapes, water-stressed crops, temperate forest and grasslands and tropical rain forests.

## 4. DIURNAL MOUNTAIN WIND SYSTEM

First, we select only the cases with **A WEAK LARGE-SCALE FORCING** (i.e.  $V_{850} < 6 \text{ m s}^{-1}$  + no synoptic fronts + precipitation<sub>day</sub> < 0.5 mm). Around 30% of the total amount of days are rejected. We plot the wind roses during different time ranges for the fair-weather days:

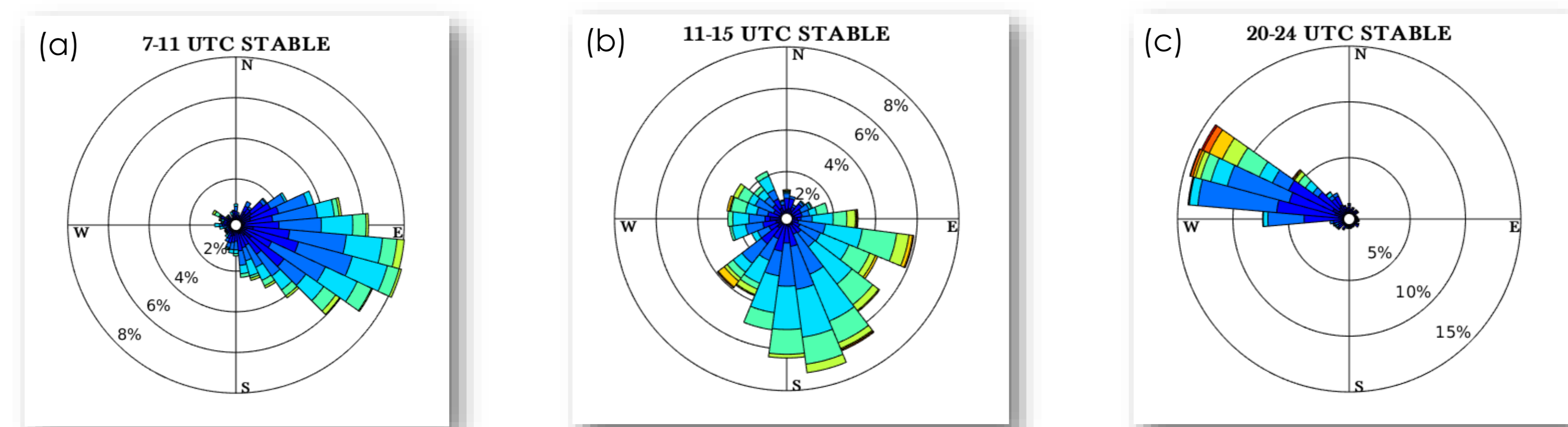


Figure 7. Wind roses for the selected large-scale stable days, (a) during UPSLOPE conditions [7-11 UTC], (b) during CENTRAL HOURS [11-15 UTC] and (c) during DOWNSLOPE conditions [20-24 UTC].

UPSLOPE/ANABATIC STAGE [70° - 160°]

UPBASIN + UPSLOPE WINDS CENTRAL HOURS: [12-14 UTC]

DOWNSLOPE/KATABATIC STAGE [250° - 340°]

We define the stages according to the wind-direction range and the mountain-range orientation.

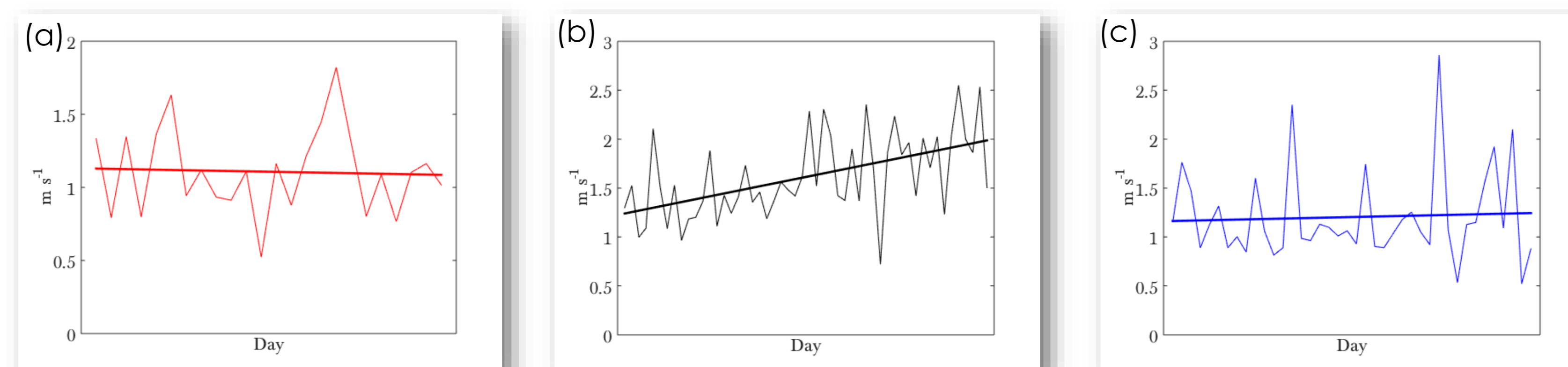


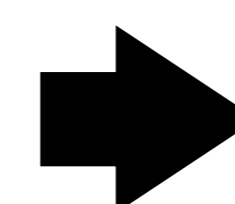
Figure 8. Evolution throughout the summer of the mean wind speed during each of the stages: (a) UPSLOPE (b) CENTRAL HOURS and (c) DOWNSLOPE. In (a) and (c) the mean wind speed is computed considering the first two hours in each direction range.

PERIOD	ANABATIC STAGE	KATABATIC STAGE
JUNE-JULY	17%	74%
AUGUST-SEPTEMBER	69%	79%

Table 1. Percentage of time in which we detect each of the stages from the total amount of days for the first part (June-July) and the second part of the summer (August-September).

HOW IS THE TURBULENCE AFFECTED?

We analyse the evolution of the friction velocity over the summer



The anabatic/upslope and katabatic/downslope intensities do not vary over the summer (Fig. 7), whereas upbasin winds intensify significantly during central hours (the increasing trend is statistically significant at the 95% confidence with a t-student test). Furthermore, the frequency of katabatics does not vary, whereas increases notably in the case of anabatics.

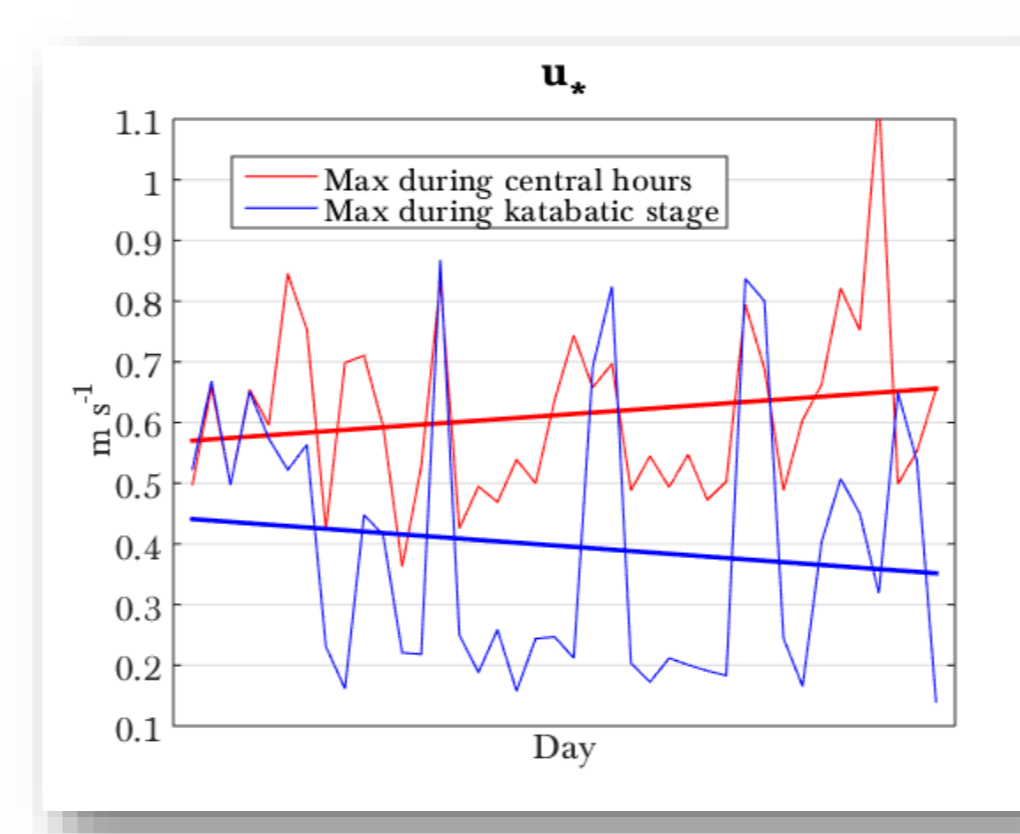


Figure 9. Evolution throughout the summer of the maximum friction velocity at the different stages during the central hours (red) and the katabatic stage (blue). The maximum friction velocity at the central hours is just represented for the days showing a clear katabatic stage.

Opposite trend throughout the summer: ≈ 0.1 m s<sup>-1</sup> increase during the central hours and decrease during the katabatic stage.

## 5. AIRPORT ISSUE

The preferential runway configuration at the airport of Madrid in summer is the North Configuration due to noise issues in close neighbourhoods. However, it has to be switched to South Configuration when the southerly winds exceed 10 knots.



Figure 10. Take off of a flight at the Adolfo Suárez Madrid-Barajas airport, with the city of Madrid at the back.

For the days with a weak large-scale forcing (stable days in Table 2), the percentage of days with runway-configuration change increases throughout the summer!

MONTH	Nº of STABLE DAYS	DAYS with CONFIGURATION change / (%)
JUNE	4	3 / 75 %
JULY	18	9 / 50 %
AUGUST	28	17 / 61 %
SEPTEMBER	10	9 / 90 %

Table 2. Number of days (absolute and percentage) in which there is a runway configuration for each month [21/06/16 – 13/09/16]

## 6. TAKE-HOME IDEAS

□ Summer 2016 was characterised for its progressive and extreme drying out of the soil.

□ Analysis of the diurnal mountain winds throughout the summer:

- Upslope/anabatic winds increase substantially in frequency but their intensity remains unchanged.
- Downslope/katabatic winds do not increase either in frequency or intensity, but the associated turbulence decreases slightly.
- The combinations of upbasin + upslope winds in central hours increases both in intensity and in the associated turbulence.

□ The wind in the central hours undergoes an intensification over the summer that induces an increase of the runway-configuration change from North to South at the airport of Madrid.

## 7. ACKNOWLEDGEMENTS

This research has been partially funded by the Spanish Government (MINECO project CGL2015-65627-C3-3-R. Jon A. Arrillaga is supported by the Predoctoral Training Program for No-Doctor Researchers of the Department of Education, Language Policy and Culture of the Basque Government (PRE\_2016\_2\_0160, MOD = B). We thank also the contribution of all the members of the GUMNet Team.